INTERNATIONAL JOURNAL of PARTICLE THERAPY

Proton Radiotherapy Could Reduce the Risk of Fatal Second Cancers for Children with Intracranial Tumors in Low- and Middle-Income Countries

Kyle J. Gallagher, PhD[1,2]; Bassem Youssef, MD[3]; Rola Georges, MS, CMD[4]; Anita Mahajan, MD[5]; Joelle Ann Feghali, MS[3]; Racile Nabha, MS[3]; Zeina Ayoub, MD[3]; Wassim Jalbout, PhD[3]; Phillip J. Taddei, PhD[3,5,6]

[1]Oregon Health and Science University, Portland, OR, USA
[2]Oregon State University, Corvallis, OR, USA
[3]American University of Beirut Medical Center, Beirut, Lebanon
[4]University of Texas MD Anderson Cancer Center, Houston, TX, USA
[5]Radiation Oncology Department, Mayo Clinic, Rochester, MN, USA
[6]University of Washington School of Medicine, Seattle, WA, USA

Abstract

Purpose: To test our hypothesis that, for young children with intracranial tumors, proton radiotherapy in a high-income country does not reduce the risk of a fatal subsequent malignant neoplasm (SMN) compared with photon radiotherapy in low- and middle-income countries.

Materials and Methods: We retrospectively selected 9 pediatric patients with low-grade brain tumors who were treated with 3-dimensional conformal radiation therapy in low- and middle-income countries. Images and contours were deidentified and transferred to a high-income country proton therapy center. Clinically commissioned treatment planning systems of each academic hospital were used to calculate absorbed dose from the therapeutic fields. After fusing supplemental computational phantoms to the patients' anatomies, models from the literature were applied to calculate stray radiation doses. Equivalent doses were determined in organs and tissues at risk of SMNs, and the lifetime attributable risk of SMN mortality (*LAR*) was predicted using a dose-effect model. Our hypothesis test was based on the average of the ratios of *LARs* from proton therapy to that of photon therapy ($\overline{RLAR}$)(H_0: $\overline{RLAR} = 1$; H_A: $\overline{RLAR} < 1$).

Results: Proton therapy reduced the equivalent dose in organs at risk for SMNs and *LARs* compared with photon therapy for which the $\overline{RLAR}$ for the cohort was 0.69 $\pm$ 0.10, resulting in the rejection of H_0 ($P < .001$, $\alpha = 0.05$). We observed that the younger children in the cohort (2-4 years old) were at a factor of approximately 2.5 higher *LAR* compared with the older children (8-12 years old).

Conclusion: Our findings suggest that proton radiotherapy has the strong potential of reducing the risk of fatal SMNs in pediatric patients with intracranial tumors if it were made available globally.

Keywords: pediatric proton therapy; intracranial tumors; secondary malignancies; global oncology; low- and middle-income countries

Submitted 03 Aug 2020
Accepted 08 Dec 2020
Published 17 Feb 2021

Corresponding Author:
Phillip J. Taddei, PhD
Radiation Oncology Department
Mayo Clinic
200 First St SW
Rochester, MN 55905, USA
Phone: +1 (507) 284-2511
taddei.phillip@mayo.edu

Original Article

DOI
10.14338/IJPT-20-00041.1

http://theijpt.org

Introduction

High long-term survival rates and sensitivity to long-term radiogenic effects for children with cancer necessitate research of late effects from cancer treatment. For children of ages 14 years and younger who have cancer, the 5-year survival rates have been reported to be 84% in the United States [1], a high-income country (HIC). One promising treatment to reduce the risk of late effects for these children globally is proton radiotherapy. In particular, proton therapy is becoming the modality of choice for pediatric patients with cancers of the central nervous system, which comprise 48% of all pediatric proton treatments [2]. However, $>$ 80% of children with cancer live in low- and middle-income countries (LMICs), with very limited access to proton therapy [3]. It has been suggested that these patients could benefit from regional proton centers [4, 5].

In HICs, for children with intracranial lesions who require radiotherapy, proton therapy is emerging as the preferred modality. Because of the enhanced radiosensitivity and close proximities of organs at risk to the treatment fields, researchers have conducted detailed dosimetric analyses of stray and therapeutic radiation [6, 7] and addressed the risk of incidence for subsequent malignant neoplasms (SMNs) [8, 9], which is the sequela of greatest concern for late fatalities [10, 11]. To our knowledge, Newhauser et al [12] were the first to observe a strong inverse relationship between the contribution to overall risk from stray radiation for a child receiving cranial scattered or scanned proton beams. In a subsequent similar study, Athar et al [8] estimated the risk of SMN incidence for 2 children with cranial lesions. They observed the risk of an SMN for intensity-modulated radiation therapy (IMRT) was less than that of passive-scattering proton therapy in tissues near the field edge but higher in tissues far from the field edge. In assessing whole-body stray radiation doses, each of those studies took advantage of the vast resources of their academic institutions to perform computationally expensive Monte Carlo simulations. Other researchers concerned about radiogenic risk of SMNs in photon and proton therapy of intracranial tumors bypassed the need for large computational resources by neglecting stray radiation contributions and considering only in-field organs at risk [9, 13]. For this reason, we decided to perform a comprehensive whole-body risk comparison between modalities for clinically realistic pediatric intracranial fields with computationally inexpensive dosimetric methods [14–16]. Further, no study had considered radiotherapy techniques that are used more globally, for example, in LMICs that are limited in their ability to implement the most advanced machinery, hardware, and software resources available in HICs.

We hypothesized that proton therapy in an HIC would provide no benefit to reducing the risk of a fatal SMN in children with intracranial tumors compared with photon therapy in an LMIC. We tested our hypothesis by performing an in silico clinical trial on a sample set of 9 pediatric patients with intracranial tumors, with sufficient statistical power. These patients were treated in an LMIC with photon therapy, and new treatment plans were created for passive-scattering proton therapy in an HIC. Equivalent dose in organs and tissues at risk of a fatal SMN (T) for each modality was calculated using the respective clinically commissioned treatment planning systems (TPSs) to estimate therapeutic radiation dose. Stray radiation dose was estimated using analytic models from the literature. The lifetime attributable risk of mortality for each SMN (LAR_{SMN}) was compared for each patient, radiogenic cancer site, and modality using a dose-effect model from the literature.

Methods

Patient sampling and contouring

Using the systematic random sampling method [17], 9 pediatric patients with promising long-term prognoses were retrospectively selected under an institutional review board protocol from ages 2 to 14 years old and were treated for low-grade intracranial tumors at a leading academic hospital in an LMIC, the American University of Beirut Medical Center. Each patient had been treated with 6-MV, 3-dimensional conformal radiation therapy (3DCRT). Computed tomography (CT) simulation images had been obtained for treatment planning from the top of the head to the neck. Missing anatomies in the CT image sets were supplemented with those of computational phantoms of matching height and weight from patients of the same sex [14]. Each patient's treatment planning data were exported to digital imaging and communications in medicine files [18] and deidentified [19]. The anonymized radiation therapy (RT) image and RT structure set files were transferred with encryption and password protection to an HIC academic hospital, the University of Texas MD Anderson Cancer Center. Target and T contours were unchanged, with the following exception. The treated volume, that is, the 95% isodose volume [20], was removed from overlapping T contours by Boolean subtraction. We chose the treated volume, rather than planning target volumes, because they were not the same size for proton and photon therapies because of differing margins. The overall set of T comprised the thyroid, red bone marrow, skin, breast tissue, lungs, liver, stomach, uterus, ovaries, prostate, bladder, colon (including the

rectum), and remainder tissues. Further information concerning the contours, the implementation of the supplemental phantoms, and the selection criteria were published previously [14].

Treatment planning and dosimetry

The calculation and distribution of dose for photon therapy treatment plans in an LMIC country used in this study were published previously [14] and are briefly described here. In that study, some treatment plans had been adjusted slightly, and all were approved by an attending pediatric radiation oncologist. A clinically commissioned commercial TPS (version 5.01, Panther, Prowess Inc, Concord, California) calculated the therapeutic absorbed dose (D) (in grays), and an analytic model from the literature [21] was reparameterized with newly measured data to estimate the out-of-field dose [14]. Equivalent dose in each voxel (H; in sieverts) was calculated as the product of absorbed dose D and the radiation weighting factor (w_R) for photons and electrons of 1 [22]. Mass-averaged mean equivalent dose in each T (H_T) was calculated for each patient and for the corresponding fused supplemental phantom. For anatomy beyond the extents of the computational phantoms, H was very low and taken as 0.

We estimated the dose distribution throughout the patients' bodies for proton therapy in the following manner. At the HIC hospital, passive-scattering proton therapy treatment plans were constructed by a proton radiotherapy dosimetrist using a clinically commissioned commercial TPS (version 8.9, Eclipse, Varian Medical Systems, Palo Alto, California). These plans were approved by an attending pediatric radiation oncologist. The TPS calculated the D from therapeutic protons. To determine H from therapeutic protons, the w_R of therapeutic protons was estimated as the approximate mean quality factor of 1.1 at any point within the fields based on linear-energy transfer, microdosimetry, and radiobiology [23–25]. To account for H from neutrons produced in the patient, an analytic model was applied as a function of distance from the field edge (ie, 50% isodose line) [15]. For H from neutrons produced in the treatment unit, an analytic model [26] was implemented with clinical adjustment factors [16]. The total equivalent dose was taken as the sum of each of those contributing radiation fields. H_T was calculated as the mass-averaged mean of the total equivalent dose in any T for each patient. Because of the minimal dosimetric effect of the few treatment plans that contained them, boost fields were omitted. All dose values were normalized to deliver a common prescribed dose (D_{Rx}) of 54 Gy and 54 Gy relative biological effectiveness (GyRBE) [27] in photon and proton therapy, respectively.

Risk of mortality from SMNs

The lifetime attributable risk of mortality for each SMN (LAR_{SMN}) was predicted using previously established methods [4] summarized below. For solid tumors, the linear no-threshold model was applied, as recommended in the *BEIR VII Report* by the National Research Council of the National Academies [28]:

$$LAR_{\mathrm{SMN}} = \frac{M_{\mathrm{SMN}}}{H_{\mathrm{ref}}} H_T, \tag{1}$$

where M_{SMN} was the lifetime age- and sex-specific risk coefficient for mortality, corresponding to each T, and H_{ref} was the reference equivalent dose of 0.1 Sv. The M_{SMN} was linearly interpolated between adjacent values of age in table 12D-2 of the *BEIR VII Report*. That table lacked M_{SMN} values for nonmelanoma skin cancer (NMSC) and thyroid cancer. For M_{NMSC}, we applied values from the International Commission on Radiological Protection (ICRP) publication 60 [23], adjusted for sex and age following methods described elsewhere [29]. For M_{thyroid}, we used the product of the incidence-risk coefficient in the *BEIR VII Report* and the lethality factor of 0.1 recommended by the ICRP publication 60 [23]. To estimate the risk from all non–site-specific solid cancers, $M_{\mathrm{othersolid}}$ and $H_{\mathrm{remainder}}$ were estimated. By postulation, the children's T received high dose and fractionated or moderate dose rates effectiveness factors reduced those M_{SMN} values by 2 for NMSC [23] and by 1.5 for all other solid tumors [28]. Our final M_{SMN} values are listed in the Supplemental Data Table S1. For LAR_{leukemia}, the hybrid approach of Taddei et al [4] was implemented. Specifically, for $H_{\mathrm{RBM}} < 2$ Sv, the no-threshold linear-quadratic model in the *BEIR VII Report* was applied, and for $H_{\mathrm{RBM}} > 2$ Sv, the quadratic term was omitted:

$$LAR_{\mathrm{leukemia}} = \begin{cases} M_{\mathrm{leukemia}} \left(\dfrac{H_{\mathrm{RBM}} + \theta H_{\mathrm{RBM}}^2}{H_{\mathrm{ref}} + \theta H_{\mathrm{ref}}^2} \right), \text{for } H_{\mathrm{RBM}} \leq 2Sv \\ M_{\mathrm{leukemia}} \left(50.7 + \dfrac{H_{\mathrm{RBM}} - 2\mathrm{Sv}}{H_{\mathrm{ref}}} \right), \text{for } H_{\mathrm{RBM}} > 2Sv \end{cases} \tag{2}$$

Table 1. Mass-averaged mean equivalent dose in each organ and tissue at risk of a fatal SMN (T) (H_T) (in sieverts) for photon therapy for each patient along with the mean (SD) of all patients [14]. Each patient is categorized according to age and sex (eg, 2-year-old male [2/M] and 2.5-year-old female [2.5/F]).

Organs and tissues	2/M	2.5/F	3/F	3.5/F	4/F	4/M	8/M	12/F	12/M	Mean (SD)
Bladder	0.058	0.071	0.017	0.027	0.021	0.060	0.014	0.013	0.019	0.033 (0.023)
Red bone marrow	3.929	4.920	3.942	4.052	6.735	5.909	2.921	3.137	1.294	4.093 (1.625)
Breast tissue	—	0.274	0.203	0.242	0.228	—	—	0.173	—	0.224 (0.038)
Liver	0.181	0.191	0.127	0.167	0.147	0.186	0.107	0.108	0.131	0.149 (0.033)
Lungs	0.286	0.277	0.188	0.239	0.210	0.300	0.197	0.205	0.229	0.237 (0.042)
Ovaries	—	0.073	0.016	0.027	0.018	—	—	0.013	—	0.029 (0.025)
Prostate	0.040	—	—	—	—	0.042	0.013	—	0.014	0.027 (0.016)
Remainder	3.824	2.097	3.059	2.271	2.110	3.323	1.297	1.130	1.210	2.258 (0.973)
Skin	1.207	1.363	1.514	0.875	1.250	1.446	0.506	0.630	0.507	1.033 (0.408)
Stomach	0.205	0.225	0.121	0.162	0.138	0.207	0.102	0.093	0.125	0.153 (0.049)
Thyroid	2.302	0.872	0.330	1.256	0.567	1.935	0.352	0.727	1.546	1.099 (0.706)
Uterus	—	0.071	0.016	0.027	0.021	—	—	0.013	—	0.030 (0.024)
Colon	0.127	0.135	0.065	0.092	0.076	0.129	0.039	0.038	0.052	0.084 (0.039)

where θ was the degree of curvature of 0.88 Sv^{-1}, and H_{ref} was 0.1 Sv. Because fatal SMNs are mutually exclusive, the following equations were used to predict the lifetime risk of any SMN mortality (LAR):

$$S = \prod_{SMN} (1 - LAR_{SMN}) \tag{3}$$

$$LAR = 1 - S \tag{4}$$

where S was the probability of avoiding all fatal SMNs (ie, of surviving SMNs). To compare the risks between the 2 modalities for a specific SMN, the ratio of LAR_{SMN} values ($RLAR_{SMN}$) was calculated for each patient as follows:

$$RLAR_{SMN} = \frac{LAR_{SMN}(\text{proton therapy})}{LAR_{SMN}(\text{photon therapy})}, \tag{5}$$

and the ratio of LAR from any SMN ($RLAR$) was calculated for each patient as follows:

$$RLAR = \frac{LAR(\text{proton therapy})}{LAR(\text{photon therapy})}. \tag{6}$$

$RLAR$ was used as a figure of merit to compare the modalities because of the lesser uncertainty than absolute risk [9, 30–33]. A one-sided t test on the mean $RLAR$ ($\overline{RLAR}$) tested our hypothesis (H_0: $\overline{RLAR} = 1$; H_A: $\overline{RLAR} < 1$; and $\alpha = 0.05$). Variances in the data were reported as one standard deviation of the mean.

Results

Equivalent dose in intracranial photon and proton therapy

Values of H_T for photon intracranial therapy are presented in Table 1 for each patient, along with average values across all patients. For photon therapy, some of these data were published previously [14]. However, unlike that study, we have removed from consideration the dose in the treated volume. Photon average $H_T > 1$ Sv, listed from largest to smallest, were in the red bone marrow, the remainder, the thyroid, and the skin. The next-highest average H_T was observed in the breast tissue of the girls and the lungs of all patients, with values > 0.2 Sv.

Values of H_T for proton intracranial therapy of the cohort are listed in Table 2. As with photon therapy, the red bone marrow received the greatest H_T. In general, organ doses were reduced in proton therapy compared with photon therapy with the exception of T located very far from the field edge (eg, ovaries or prostate) for which doses were comparable but small (< 0.02 Sv difference). In proton therapy, only the red bone marrow and remainder tissues received an H_T of > 1 Sv. For the thyroid and skin, average H_T ranged between 0.2 and 1 Sv. Finally, average H_T in the breast tissues of the girls and the lungs of all patients was < 0.2 Sv.

Table 2. Mass-averaged mean equivalent dose in each organ and tissue at risk of a fatal SMN (T) (H_T) (in sieverts) for proton therapy for each patient along with the mean (SD) of all patients [14]. Each patient is abbreviated according to age and sex (eg, 2-year-old male [2/M] and 2.5-year-old female [2.5/F]).

Organs and tissues	2/M	2.5/F	3/F	3.5/F	4/F	4/M	8/M	12/F	12/M	Mean (SD)
Bladder	0.062	0.043	0.036	0.023	0.038	0.057	0.027	0.021	0.047	0.039 (0.014)
Red bone marrow	3.875	2.993	3.838	2.292	5.208	2.821	1.586	2.428	0.751	2.866 (1.327)
Breast tissue	—	0.134	0.187	0.093	0.162	—	—	0.132	—	0.142 (0.035)
Liver	0.124	0.091	0.115	0.059	0.101	0.123	0.075	0.092	0.118	0.100 (0.022)
Lungs	0.204	0.138	0.194	0.076	0.134	0.191	0.127	0.171	0.213	0.161 (0.045)
Ovaries	—	0.043	0.036	0.019	0.034	—	—	0.025	—	0.031 (0.009)
Prostate	0.053	—	—	—	—	0.050	0.024	—	0.046	0.043 (0.013)
Remainder	2.491	1.493	1.956	1.167	1.564	1.804	0.746	0.936	0.857	1.446 (0.578)
Skin	1.107	0.977	1.649	1.522	1.001	0.839	0.253	0.536	0.516	0.933 (0.461)
Stomach	0.132	0.097	0.104	0.055	0.094	0.111	0.062	0.081	0.106	0.094 (0.024)
Thyroid	0.318	0.211	0.763	0.155	0.304	0.276	0.251	0.634	0.436	0.372 (0.203)
Uterus	—	0.043	0.036	0.018	0.033	—	—	0.024	—	0.031 (0.010)
Colon	0.090	0.065	0.068	0.042	0.068	0.078	0.041	0.044	0.069	0.063 (0.017)

Predicted risk of a fatal SMN

The average LAR_{SMN} values for photon therapy are plotted in Figure 1. The cancer sites with the highest LAR_{SMN} were other solid tumors and leukemia, for which the average LAR_{SMN} values were $>$ 4%. Moderate values of LAR_{SMN}—between 0.1% and 1%—were found for lung and thyroid cancers in each patient and fatal breast cancer in the girls. We compared values of LAR in terms of age and sex. The mean LAR for the younger children (ie, those 2-4 years old), at 15.6% (1.9%), was higher than that of the older children (ie, those 8-12 years old), at 6.3% (1.5%). Between sexes, we did not observe a significant difference in the average LAR for photon therapy for the girls, at 13.0% (3.6%), or boys, at 11.8% (6.7%). These data are listed in Supplemental Data Table S2.

Similar trends in LAR_{SMN} and LAR for photon therapy were observed in proton therapy. The cancer sites with the highest average LAR_{SMN} for proton therapy were solid tumors and leukemia, each $>$ 3%. Although reduced in proton therapy, moderate risks of late fatalities between 0.1% and 1% were observed for lung and thyroid cancers in each child and breast cancer in the girls. To approximate pencil-beam-scanning proton therapy, stray radiation dose from external neutrons was set to zero [15, 34–36]. In this case, moderate values of LAR_{SMN} for fully out-of-field organs and tissues decreased to $<$ 0.1%. However, even in that case, the high risks from solid tumors and leukemia were maintained. With respect to age, the average LAR in proton therapy was increased for the younger children, at 10.7% (2.2%), compared with that of the older children, at 4.4% (1.4%). Finally, no significant differences were observed between the sexes for which the average LAR values were 9.3% (2.6%) for the girls and 7.8% (5.0%) for the boys. These data are listed in Supplemental Data Table S3.

The $RLAR_{SMN}$ values, averaged across all 9 patients, are shown for each T in Figure 2. The $RLAR$ was $<$ 1 for each patient. The smallest mean $RLAR_{SMN}$ was 0.60 (0.70) for thyroid cancer. With 4 exceptions, the average $RLAR_{SMN}$ values were $<$ 1, indicating an advantage for proton therapy in an HIC. The exceptions were bladder cancer, ovarian and uterine cancers in girls, and prostate cancer in boys. However, the absolute LAR_{SMN} values for those cancer sites were negligible, on average $<$ 0.02%, for either proton or photon therapy. Regarding relationships between $RLAR$ and age or sex, no significant differences were observed. These data are listed in Supplemental Data Table S4. Overall, for this cohort, the 1-sided t test resulted in the rejection of the null hypothesis with $P < .001$, and $\overline{RLAR}$ was 0.69 $\pm$ 0.10. The value of $\overline{RLAR}$ was reduced to 0.58 $\pm$ 0.09 if external neutrons were omitted as an approximation of pencil-beam-scanning proton therapy.

Discussion

In this in silico, virtual trial, we tested the hypothesis that no improvement in minimizing the risk of a fatal SMN would result from treating pediatric patients with intracranial tumors with proton therapy in an HIC rather than photon therapy in an LMIC. Our hypothesis was rejected with statistical significance, and our results suggest that proton therapy offered in HICs, if distributed to LMICs, could reduce the risk of fatal SMNs. Specifically, for a sample set of young children, the average (SD)

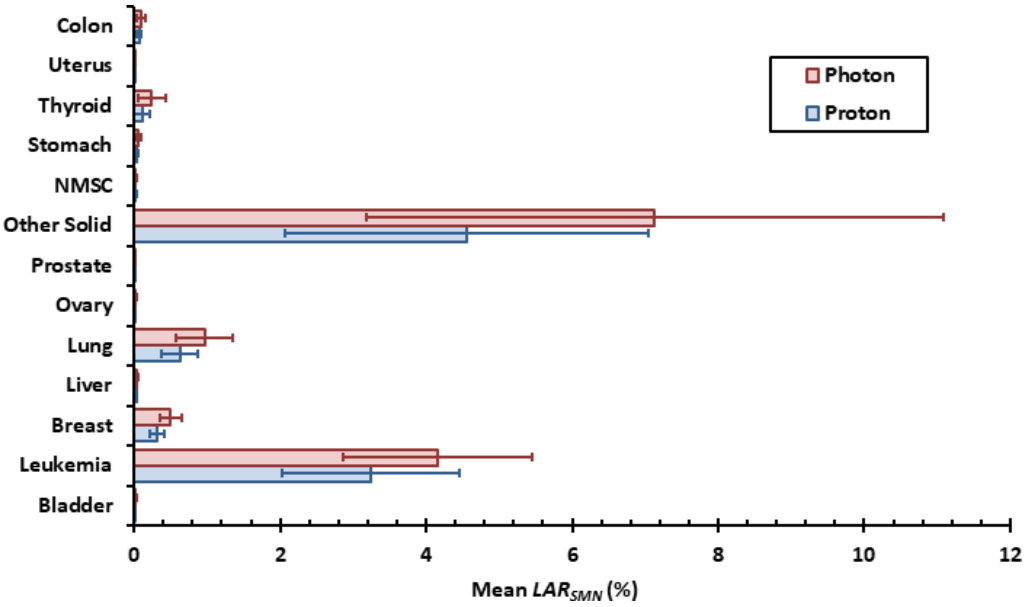

Figure 1. LAR_{SMN} values for photon (red) and proton (blue) therapies for each cancer site averaged across all patients. Error bars represent 1 SD of the mean.

predicted total *RLAR* for the cohort was 0.69 (0.10) ($P < .001$). The fatal SMNs of greatest concern in either modality were leukemia and other solid tumors; for which, the potential reductions in risks were 23% and 34%, respectively. Younger children were at heightened risk versus older children by approximately a factor of 2.5, and no difference was observed between girls and boys. It should be noted that these observations were based on small sample sets of each subgroup and, therefore, warrant further investigation. The advantage of proton therapy was pronounced when eliminating secondary neutron dose from the treatment unit, an approximation to pencil-beam-scanning proton therapy, even without considering the improved proximal conformity in that modality.

Some fatal SMN sites resulted in greater relative risk reductions than others. For example, the risk of a fatal thyroid cancer was reduced by 40% for proton therapy. However, the absolute risk of a fatal thyroid cancer was small, which showed that it is important in comparative studies to report absolute risk and not merely ratios of risks. Other cancer sites with > 20% reduction

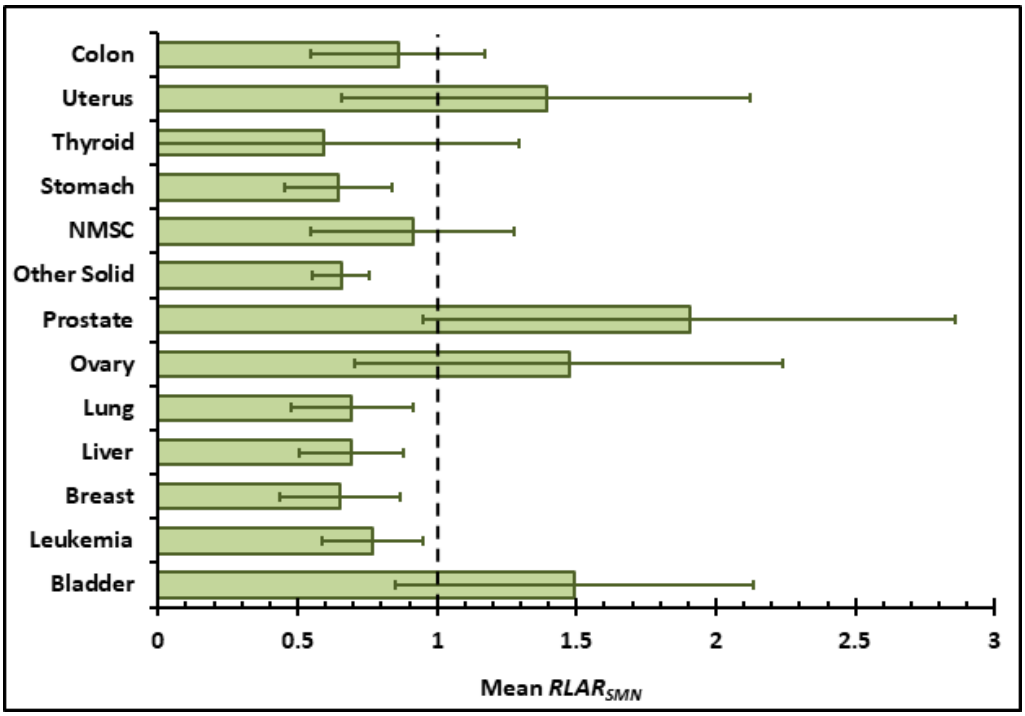

Figure 2. $RLAR_{SMN}$ values for each cancer site averaged across all patients. Error bars represent 1 SD of each mean.

in risk for an HIC proton therapy versus an LMIC photon therapy included other solid tumors, leukemia, lung, breast, liver, and stomach cancers, which comprised the primary contributors to the absolute risks of a fatal SMN.

In *T* associated with fatal SMNs that may develop within or near the field edge, proton therapy reduced the dose compared with photon therapy. In *T* located far from the composite field edges, the predicted absolute LAR_{SMN} values in 3DCRT or proton therapy were small at $< 0.02\%$ on average. This slightly lower dose from photon therapy was likely influenced by (intentionally) applying low-energy photon beams with photonuclear cross sections that are colloquially assumed as zero and a widely accepted, lower out-of-field dose in 3DCRT than IMRT by a factor of 3 to 5 [37, 38]. This finding indicates that these incremental risks are negligible compared with other risks survivors of childhood cancer face, and future clinical or research studies should consider omitting them. For the approximation of pencil-beam scanning, proton therapy reduced the dose to all organs at risk compared with photon therapy.

The nearest matches in patients within our cohort and that of Athar et al [8] were their 8-year-old girl and 14-year-old boy. In both studies, pencil-beam-scanning proton therapy reduced the risk for all organs compared with photon therapy. However, they observed that organs near the field edge had lower predicted risk using photon therapy compared with passive-scattering proton therapy and higher risk far from the field edge. Conversely, we predicted that passive-scattering proton therapy had comparable risk to that of photon therapy far from the field edge. This difference may have been because our study's clinical 3DCRT fields differed from their circular IMRT treatment fields to match the proton fields. In addition, Athar et al predicted the risk of incidence, whereas we predicted the risk of fatality. Considering that and other reasonable small variations between the studies, the findings of the 2 studies were in good agreement.

Predicted risks may be compared with findings of relevant epidemiologic studies. Although there have been no long-term follow-up studies for proton therapy, there have been several for photon therapy. The largest such study in the United States is the Childhood Cancer Survivor Study. In that study, at 30 years of follow-up, a 2.8% rate of fatal SMNs was observed in 2881 patients treated with photon radiotherapy for central nervous system (CNS) cancers [10]. Our larger predicted lifetime risks of a fatal SMN (mean [SD], 12.5% [4.9%]) may be attributed to the following. First, 30 years is insufficient to assess lifetime risk for survivors of childhood cancer. Second, the other study was managed by self-reporting, which may result in an underestimation of the actual prevalence. Third, the other study's cohort was older in age compared with the children in our study, and, as with the epidemiologic study, we found that younger children were at greater risk than older children. These findings indicate that, over their lifetimes, the rate of fatal SMNs will continue to grow in survivors of childhood cancer, especially those who have received radiotherapy.

Our in silico trial required whole-body dosimetry in regions lacking anatomic data. As a model for future clinical or research studies, these novel methods can reduce computational overhead and enable cohorts to be examined for extensive healthy tissue dosimetry, even for CT extents that omit patient-specific anatomic data. Here, we demonstrated the feasibility of applying automated methods to computer codes that could attach to commercial proton and photon therapy TPSs to supplement the existing therapeutic doses with stray-radiation dose estimates. Furthermore, running analytic models, rather than Monte Carlo simulations, greatly reduced the computational overhead of such studies. This may allow researchers and clinicians to routinely compare different modalities or optimize treatment plans with specific consideration to long-term morbidities or mortalities. By extending the anatomies of the patients and applying these analytic models, we were able to estimate dose throughout the children's bodies and to predict risks of all radiogenic cancer sites.

Our study had the following limitations. As with any study predicting the risks of late sequelae, the inherent systematic uncertainties in the risk model were large and have yet to be fully quantified. Those uncertainties are attributable mainly to the risk model and not to physical dose calculations. The main factors that contribute to uncertainties include dose and dose rate effects, the transfer between historic Japanese and other populations, and the sampling variability in the model's parameter estimates [28]. Even so, a review of epidemiology data revealed that risk models derived from the cohort of Japanese survivors of the atomic bomb were generally in agreement with carcinogenesis from fractionated high-dose exposures [39]. To minimize the effect of systematic uncertainties in the risk model, we used the ratio of the risks as a figure of merit to test our hypothesis.

The LMICs have limited resources, which present unique environment-specific challenges in providing advanced radiotherapy technologies. Those complexities include added expense, proton-specific expertise, and upgraded facilities and software [40]. For example, patients with CNS tumors at our LMIC institution generally receive radiotherapy with the 3DCRT technique, rather than with IMRT, even though the latter is widely considered to be superior and results in dose distributions that are more conformal [41, 42]. Because of a paucity of robust studies to show true clinical improvement in oncologic outcomes or toxicities to healthy tissues and the associated supplemental cost for CNS tumors, even in this upper-middle-

income country, most payers do not reimburse for IMRT. On the other hand, recently Russia, India, and China have all emerged as LMICs that have integrated regional centers for particle therapy into their oncology care.

In conclusion, for a small cohort of young pediatric patients with intracranial tumors, we found with statistical significance that our hypothesis was rejected. Specifically, proton therapy in an HIC reduced the risk of a fatal SMN compared with the risk from photon therapy in an LMIC. This finding implies that, if regional proton therapy centers were commissioned in LMICs, then children with brain cancer could benefit. Our methods were repeatable in estimating equivalent dose in organs at risk throughout the whole body using analytic models and supplemental phantoms. We recommend that they be applied to enable further clinical and research studies of this type, including those of larger cohorts [43, 44], with the purpose of minimizing long-term side effects in survivors of childhood cancer.

ADDITIONAL INFORMATION AND DECLARATIONS

Conflicts of Interest: Anita Mahajan, MD, is an Associate Editor of the *International Journal of Particle Therapy*. The authors have no additional conflicts of interest to disclose.

Acknowledgments: The authors wish to thank Dr Toufic Eid for his scientific and clinical contributions to this study. The content of this study is solely the responsibility of the authors.

Funding: This research was supported in part by the Fogarty International Center (award K01TW008409), the Naef K. Basile Cancer Institute, and the Portland Chapter of the Achievement Rewards for College Scientists.

Ethical Approval: All patient data were collected under internal review board–approved protocol.

References

1. American Cancer Society. Cancer facts & figures 2020. https://www.cancer.org/research/cancer-facts-statistics/all-cancer-facts-figures/cancer-facts-figures-2020.html. Published 2020. Accessed March 9, 2020.
2. Journy N, Indelicato DJ, Withrow DR, Akimoto T, Alapetite C, Araya M, Chang A, Chang JH, Chon B, Confer ME, Demizu Y, Dendale R, Doyen J, Ermoian R, Gurtner K, Hill-Kayser C, Iwata H, Kim JY, Kwok Y, Laack NN, Lee C, Lim DH, Loredo L, Mangona VS, Mansur DB, Murakami M, Murayama S, Ogino T, Ondrová B, Parikh RR, Paulino AC, Perkins S, Ramakrishna NR, Richter R, Rombi B, Shibata S, Shimizu S, Timmermann B, Vern-Gross T, Wang CJ, Weber DC, Wilkinson JB, Witt Nyström P, Yock TI, Kleinerman RA, Berrington de Gonzalez A. Patterns of proton therapy use in pediatric cancer management in 2016: an international survey. *Radiother Oncol*. 2019;132:155–61.
3. American Cancer Society. Global cancer facts & figures. 4th ed. https://www.cancer.org/research/cancer-facts-statistics/global.html. Published 2018. Accessed March 9, 2020.
4. Taddei PJ, Khater N, Youssef B, Howell RM, Jalbout W, Zhang R, Geara FB, Giebeler A, Mahajan A, Mirkovic D, Newhauser W. Low- and middle-income countries can reduce risks of subsequent neoplasms by referring pediatric craniospinal cases to centralized proton treatment centers. *Biomed Phys Eng Express*. 2018;4:025029.
5. Taddei PJ, Khater N, Zhang R, Geara FB, Mahajan A, Jalbout W, Pérez-Andújar A, Youssef B, Newhauser WD. Inter-institutional comparison of personalized risk assessments for second malignant neoplasms for a 13-year-old girl receiving proton versus photon craniospinal irradiation. *Cancers (Basel)*. 2015;7:407–26.
6. Matsumoto S, Koba Y, Kohno R, Lee C, Bolch WE, Kai M. Secondary neutron doses to pediatric patients during intracranial proton therapy: Monte Carlo simulation of the neutron energy spectrum and its organ doses. *Health Phys*. 2016;110:380–6.
7. Sayah R, Farah J, Donadille L, Hérault J, Delacroix S, De Marzi L, De Oliveira A, Vabre I, Stichelbaut F, Lee C, Bolch WE, Clairand I. Secondary neutron doses received by paediatric patients during intracranial proton therapy treatments. *J Radiol Prot*. 2014;34:279–96.
8. Athar BS, Paganetti H. Comparison of second cancer risk due to out-of-field doses from 6-MV IMRT and proton therapy based on 6 pediatric patient treatment plans. Radiother Oncol. 2011;98:87–92.
9. Moteabbed M, Yock TI, Paganetti H. The risk of radiation-induced second cancers in the high to medium dose region: a comparison between passive and scanned proton therapy, IMRT and VMAT for pediatric patients with brain tumors. *Phys Med Biol*. 2014;59:2883–99.
10. Armstrong GT. Long-term survivors of childhood central nervous system malignancies: the experience of the Childhood Cancer Survivor Study. *Eur J Paediatr Neurol*. 2010;14:298–303.

11. Armstrong GT, Liu Q, Yasui Y, Neglia JP, Leisenring W, Robison LL, Mertens AC. Late mortality among 5-year survivors of childhood cancer: a summary from the Childhood Cancer Survivor Study. *J Clin Oncol*. 2009;27:2328–38.
12. Newhauser WD, Fontenot JD, Mahajan A, Kornguth D, Stovall M, Zheng Y, Taddei PJ, Mirkovic D, Mohan R, Cox JD, Woo S. The risk of developing a second cancer after receiving craniospinal proton irradiation. *Phys Med Biol*. 2009;54: 2277–91.
13. Paganetti H, Athar BS, Moteabbed M, Adams JA, Schneider U, Yock TI. Assessment of radiation-induced second cancer risks in proton therapy and IMRT for organs inside the primary radiation field. *Phys Med Biol*. 2012;57:6047–61.
14. Gallagher KJ, Tannous J, Nabha R, Feghali JA, Ayoub Z, Jalbout W, Youssef B, Taddei PJ. Supplemental computational phantoms to estimate out-of-field absorbed dose in photon radiotherapy. *Phys Med Biol*. 2018;63:025021.
15. Gallagher KJ, Taddei PJ. Analytical model to estimate equivalent dose from internal neutrons in proton therapy of children with intracranial tumors. *Radiat Prot Dosimetry*. 2019;183:459–67.
16. Gallagher KJ, Taddei PJ. Independent application of an analytical model for secondary neutron equivalent dose produced in a passive-scattering proton therapy treatment unit. *Phys Med Biol*. 2018;63:15NT04.
17. Lunsford T, Lunsford B. The research sample, part I: sampling. *J Prosthet Orthot*. 1995;7:105–12.
18. Law MYY, Liu B. Informatics in radiology: DICOM-RT and its utilization in radiation therapy. *Radiographics*. 2009;29:655–67.
19. Newhauser W, Jones T, Swerdloff S, Newhauser W, Cilia M, Carver R, Halloran A, Zhang R. Anonymization of DICOM electronic medical records for radiation therapy. *Comput Biol Med*. 2014;53:134–40.
20. International Commission on Radiation Units and Measurements. ICRU Report 50: Prescribing, Recording, and Reporting Photon Beam Therapy: 1993. URL: https://icru.org/home/reports/prescribing-recording-and-reporting-photon-beam-therapy-report-50. Accessed December 1, 2015.
21. Taddei PJ, Jalbout W, Howell RM, Khater N, Geara F, Homann K, et al. Analytical model for out-of-field dose in photon craniospinal irradiation. Phys Med Biol 2013;58:7463–79.
22. International Commission on Radiological Protection. *The 2007 Recommendations of the International Commission on Radiological Protection*. Published 2007. Accessed December 1, 2015. *ICRP Publication 103*. http://www.icrp.org/publication.asp?id=ICRP%20Publication%20103.
23. International Commission on Radiological Protection. *1990 Recommendations of the International Commission on Radiological Protection*. Published 1991. Accessed December 1, 2015. *ICRP Publication 60*. https://www.icrp.org/publication.asp?id=ICRP%20Publication%2060.
24. International Commission on Radiation Units and Measurements. *Stopping Powers and Ranges for Protons and Alpha Particles*. Published 1993. Accessed December 1, 2015. *ICRU Report 49*. https://icru.org/home/reports/stopping-power-and-ranges-for-protons-and-alpha-particles-report-49.
25. Robertson JB, Eaddy JM, Archambeau JO, Coutrakon GB, Miller DW, Moyers MF, Siebers JV, Slater JM, Dicello JF. Variation of measured proton relative biological effectiveness (RBE) as a function of initial proton energy. In: Amaldi U, Larsson B, eds. *Hadrontherapy in Oncology: Proceedings of the First International Symposium on Hadrontherapy* (Como, Italy, 18–21 October 1993). Amsterdam, the Netherlands: Elsevier;1994;132:66–72.
26. Schneider C, Newhauser W, Farah J. An analytical model of leakage neutron equivalent dose for passively-scattered proton radiotherapy and validation with measurements. *Cancers (Basel)*. 2015;7:795–810.
27. International Commission on Radiation Units and Measurements. *Prescribing, Recording, and Reporting Proton-Beam Therapy*. Published 2007. Accessed December 1, 2015. *ICRU Report 78*. https://icru.org/home/reports/prescribing-recording-and-reporting-proton-beam-therapy-icru-report-78.
28. National Research Council. *Health Risks from Exposure to Low Levels of Ionizing Radiation: BEIR VII Phase 2*. Published 2006. Accessed December 1, 2015. https://www.nap.edu/catalog/11340/health-risks-from-exposure-to-low-levels-of-ionizing-radiation.
29. Taddei PJ, Mahajan A, Mirkovic D, Zhang R, Giebeler A, Kornguth D, Harvey M, Woo S, Newhauser WD. Predicted risks of second malignant neoplasm incidence and mortality due to secondary neutrons in a girl and boy receiving proton craniospinal irradiation. *Phys Med Biol*. 2010;55:7067–80.
30. Nguyen J, Moteabbed M, Paganetti H. Assessment of uncertainties in radiation-induced cancer risk predictions at clinically relevant doses. *Med Phys*. 2015;42:81–9.

31. Zhang R. *Quantitative Comparison of Late Effects following Photon versus Proton External-Beam Radiation Therapies: Toward an Evidence-Based Approach to Selecting a Treatment Modality* [dissertation]. Houston, TX: University of Texas Health Graduate School of Biomedical Sciences; 2011.
32. Fontenot JD, Bloch C, Followill D, Titt U, Newhauser WD. Estimate of the uncertainties in the relative risk of secondary malignant neoplasms following proton therapy and intensity-modulated photon therapy. *Phys Med Biol*. 2010;55:6987–98.
33. Kry SF, Followill D, White RA, Stovall M, Kuban DA, Salehpour M. Uncertainty of calculated risk estimates for secondary malignancies after radiotherapy. *Int J Radiat Oncol Biol Phys*. 2007;68:1265–71.
34. Hälg RA, Schneider U. Neutron dose and its measurement in proton therapy—current state of knowledge. *Br J Radiol*. 2020;93:20190412.
35. Schneider U, Agosteo S, Pedroni E, Besserer J. Secondary neutron dose during proton therapy using spot scanning. *Int J Radiat Oncol*. 2002;53:244–51.
36. Stolarczyk L, Trinkl S, Romero-Expósito M, Mojżeszek N, Ambrozova I, Domingo C, Davídková M, Farah J, Kłodowska M, Knežević Ž, Liszka M, Majer M, Miljanić S, Ploc O, Schwarz M, Harrison RM, Olko P. Dose distribution of secondary radiation in a water phantom for a proton pencil beam-EURADOS WG9 intercomparison exercise. *Phys Med Biol*. 2018; 63:085017.
37. Hall EJ, Wuu CS. Radiation-induced second cancers: the impact of 3D-CRT and IMRT. *Int J Radiat Oncol Biol Phys*. 2003;56:83–8.
38. Kry SF, Bednarz B, Howell RM, Dauer L, Followill D, Klein E, Paganetti H, Wang B, Wuu CS, George Xu X. AAPM TG 158: Measurement and calculation of doses outside the treated volume from external-beam radiation therapy. *Med Phys*. 2017;44:e391–429.
39. Berrington de Gonzalez AB, Gilbert E, Curtis R, Inskip P, Kleinerman R, Morton L, Rajaraman P, Little MP. Second solid cancers after radiotherapy: a systematic review of the epidemiological studies of the radiation dose-response relationship. *Int J Radiat Oncol Biol Phys*. 2013;86:224–33.
40. Rosenblatt E, Meghzifene A, Belyakov O, Abdel-Wahab M. Relevance of particle therapy to developing countries. *Int J Radiat Oncol Biol Phys*. 2016;95:25–9.
41. Takizawa D, Mizumoto M, Yamamoto T, Oshiro Y, Fukushima H, Fukushima T, Terunuma T, Okumura T, Tsuboi K, Sakurai H. A comparative study of dose distribution of PBT, 3D-CRT and IMRT for pediatric brain tumors. *Radiat Oncol*. 2017;12:40.
42. Lee CT, Bilton SD, Famiglietti RM, Riley BA, Mahajan A, Chang EL, Maor MH, Woo SY, Cox JD, Smith AR. Treatment planning with protons for pediatric retinoblastoma, medulloblastoma, and pelvic sarcoma: how do protons compare with other conformal techniques? *Int J Radiat Oncol Biol Phys*. 2005;63:362–72.
43. Newhauser WD, de Gonzalez AB, Schulte R, Lee C. A review of radiotherapy-induced late effects research after advanced technology treatments. *Front Oncol*. 2016;6:13.
44. Stokkevåg CH, Schneider U, Muren LP, Newhauser W. Radiation-induced cancer risk predictions in proton and heavy ion radiotherapy. *Phys Med*. 2017;42:259–62.